

Monte Carlo Studies on Proton Computed Tomography using a Silicon Strip Detector Telescope

L. R. Johnson*, B. Keeney*, G. Ross*, H. F.-W. Sadrozinski* (Senior member, IEEE),
A. Seiden*, D. C. Williams*, L. Zhang*
V. Bashkirov†, R. W. Schulte †, K Shahnazi †

*Santa Cruz Institute for Particle Physics, UC Santa Cruz, CA 95064

†Loma Linda University Medical Center, Loma Linda, CA 92354

Abstract— Monte Carlo computer programs such as the GEANT4 toolkit include precise models of particle interactions and can be an invaluable tool for studying the feasibility of new imaging techniques such as proton computed tomography (pCT). Presented in this paper is a comparison of laboratory data with GEANT4 predictions for the imaging characteristics of a simple metal object using a particle beam and a silicon particle detector.

I. INTRODUCTION

Computed tomography (CT) has become an important tool in medical imaging. Reconstruction methods allow doctors to make detailed pictures of everything from the brain to the heart. CT is especially important in imaging irregular growths or damaged and diseased tissue for treatment purposes. However, traditional CT scans using X-rays as probes have a disadvantage of a relatively high radiation dosage. A possible alternative is proton computed tomography (pCT), an imaging technique that substitutes protons for X-rays. Imaging with protons could have the advantage of providing similar quality reconstruction with much less dose. [13]

In order to study the feasibility of pCT or other alternative imaging techniques, it is important to be able to understand the proton transmission images seen in the lab. An accurate analysis of laboratory data requires the use of detailed computer simulations. GEANT4 is an excellent tool for this purpose [7]. In this paper we will examine the correlation between laboratory data and GEANT4 simulations.

II. EXPERIMENT

A. Setup

Data for our initial experiments was taken using the medical proton synchrotron at Loma Linda University Medical Center. A monochromatic beam of 250 MeV protons is degraded by a 25.4 cm thick wax block, resulting in protons with mean energy of approximately 130 MeV. The protons then pass through a 5.0 cm long aluminum tube (outer diameter OD = 3.0 cm, inner diameter ID = 0.68 cm) resting on a polystyrene holder and placed 25 cm behind the wax block. The protons were then detected by two sets of silicon strip detectors (SSD), one placed directly behind the tube, and the second 27.3 cm from the first as shown in Figure 1.

The wax material of the beam degrader has a physical density of $0.926\text{g}/\text{cm}^3$. The water-equivalent thickness in terms of proton stopping power is 0.981 cm (1 cm wax = 0.981 cm water) for high energy protons. The elemental composition of the wax was described in [12], and is very close to that of polyethylene, which is, by weight, 0.143711 H and 0.856289 C.

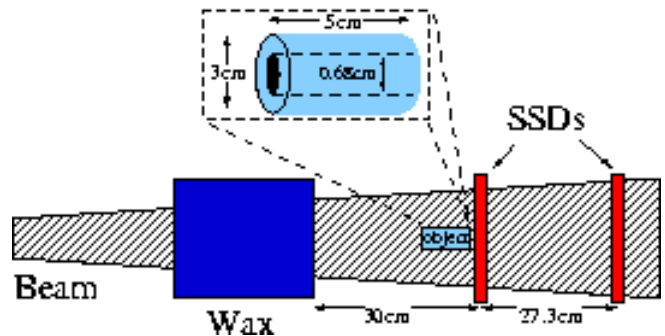


Fig. 1. Experimental setup used for the study of Proton Computed Tomography (pCT).

Each SSD consists of a pair of single-sided silicon strip detectors, originally developed for the gamma-ray large area space telescope (GLAST). [3] Each single-sided detector is composed of 320 thin strips of silicon aligned parallel to each other in a plane. In each detector plane, two of these single sided detectors are arranged such that they have orthogonal strip orientation. The detectors are $400\ \mu\text{m}$ thick, with a pitch of 194 microns, and outer dimensions of 6.4 cm by 6.4 cm. These detectors measure the trajectory of the protons (incident x and y position and direction) as well as their energy. The first is determined from strip-hit information, and the latter by measuring the charge deposited in the detector. [11]

B. Energy Measurement

For each event there are three kinds of quantities recorded: event number, strip hit information for each detector, and time over threshold (TOT). The strip hit information tells which strips in the SSD are traversed by protons. Since each detector plane contains two silicon detectors with strips oriented in perpendicular directions, both x and y trajectories can be measured with high precision.

As protons pass through the detector, they deposit some amount of charge in the silicon that depends on the energy of the proton. This energy creates a signal which is transmitted to a binary chip with a threshold that can be set for every channel, and has a fast output of TOT. The TOT depends linearly on the input charge up to about 100 fC. By using specific proton energies and measuring the corresponding TOT, an experimental calibration curve was obtained. This curve, shown in Figure 2, was used to calculate the proton energies from TOT in our experiment. [11]

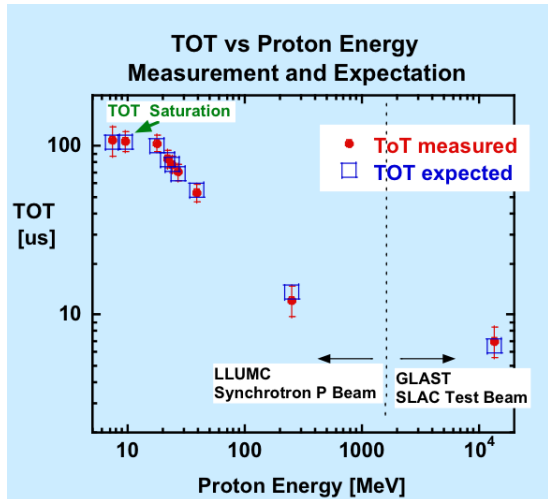


Fig. 2. By using specific proton energies and measuring the corresponding time over threshold (TOT), this experimental calibration curve was obtained. It was used to calculate the proton energies from TOT in our experiment.

In the process of recording the data, certain events were excluded from analysis. One feature of the integrated circuit used for the readout¹ is that it only returns one TOT value per detector regardless of how many strips are hit. Multiple-hit events are generally from individual protons passing through an area at the edge of two strips in a plane, in which case the deposited charge is shared between strips. Therefore, in order to get good energy resolution, we exclude any events that activated more than one strip per plane. The resulting average energy vs position measurements are shown in Figure 3.

III. SIMULATION

The Monte Carlo simulation program GEANT4 was used to model our simple experimental setup. GEANT4 was developed by RD44 with the goal of providing a toolkit to simulate the passage of particles through matter. Although GEANT4 was primarily intended (and tested) for the simulation of high-energy physics experiments, it can be applied to a wide variety of applications, including medical physics. For this reason, it is

¹The circuit used here was designed for GLAST [10]. It is a low-power design meant for use in a satellite. An amplifier custom designed for the pCT application is currently in development as a replacement.

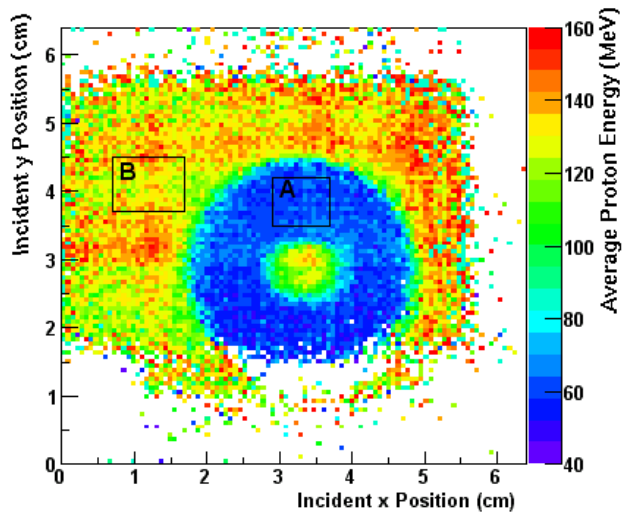


Fig. 3. Experimentally observed proton energy, converted from the TOT values, and including multiple-hit cuts and chip calibration.

important to verify its accuracy at the types of energies useful for pCT. [1]

The parameters for the simulation were matched to the physical setup described in Section II-A. The simulated beam consisted of 250 MeV monochromatic protons. The dimensions for the wax block, aluminum tube and silicon detectors were identical to the experimental setup, as were the alignment and spacing of these objects. The wax was modeled as a simple solid made of 85.6% carbon, 14.4% hydrogen, with density $\rho = 0.926g/cm^3$. Each detector was modeled as two thin sheets of silicon adjacent to each other. At the plane of the detector, the energy, x and y positions and incident angle were recorded for each proton. The data was then analyzed in a manner similar to the experimental data.

IV. COMPARISON OF EXPERIMENT WITH MONTE CARLO

A. Multiple Scattering

As particles travel through matter, they interact primarily with nuclei via the Coulomb interaction, and scatter. If the material is thick enough, many small deflections combine to produce scattering angles in a Gaussian distribution of predictable width:

$$\theta_0 \propto \frac{z\sqrt{x/X_0}}{\beta cp} \quad (1)$$

Here, p is the momentum, βc the velocity, z the charge number of the incident particle and x/X_0 is the thickness of the medium in radiation lengths. [4] We would expect to see this Gaussian behavior in both the data and the simulation.

For this measurement, we relaxed the requirement of only one hit per plane discussed in Section II-B. This is to avoid bias, since particles traveling at an angle are more likely to hit

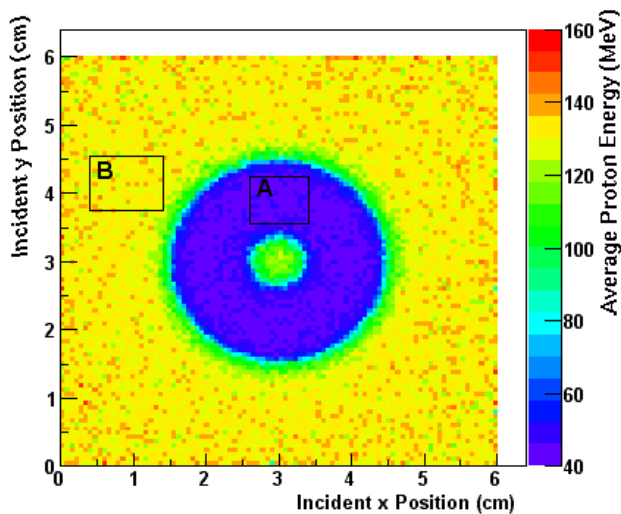


Fig. 4. Simulated proton energy vs. position without cuts.

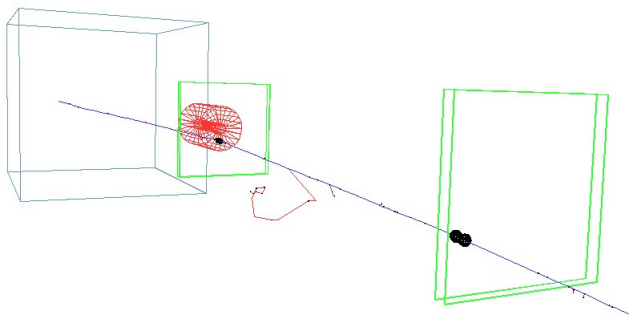


Fig. 5. T-D image of one simulated proton being scattered by the wax and aluminum tube, generated using GEANT4. The wax is the large box, the single sided SSDs are shown in green, the aluminum tube in red. The points where the proton impacted the detectors are shown in black. The red lines are secondary particles created by GEANT4 (delta rays).

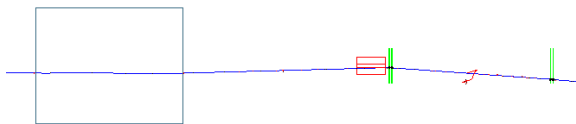


Fig. 6. Two-D side view of event in Figure 5. It is easy to see the angle of deflection between the incident proton and the final path after it has passed through the aluminum tube.

multiple strips. In order to extract information about the multiple scattering of the protons in the experimental setup, it was important to be able to match events in the first and second detector planes. By comparing the x and y position of the proton hit in the first plane to the position in the second plane, the incident angle from the norm was extracted and recorded.

In running the simulation, one of the parameters recorded for

each proton was the incident angle at the plane of the first detector. However, in order to compare the simulation with experiment it is important to make the same set of cuts on the both sets of data. Therefore we required that the "good" events in the simulation must also impact both detector planes. This then excluded any protons that scatter with an angle large enough to miss the second detector.

We compared scattering data for protons that passed through the aluminum tube (region A in Figures 3 and 4) separately from scattering data for protons that did not pass through the aluminum (region B in Figures 3 and 4). The comparisons for each region are shown in Figure 7.

There is good agreement between the experimental and simulated results. Both distributions are roughly Gaussian in shape, and centered at zero. The spread in scattering angles in region A is significantly wider than the spread in region B. This is expected, since the scattering angle depends on the amount and density of material traversed. GEANT4 appears to accurately simulate multiple scattering for protons at these energies.

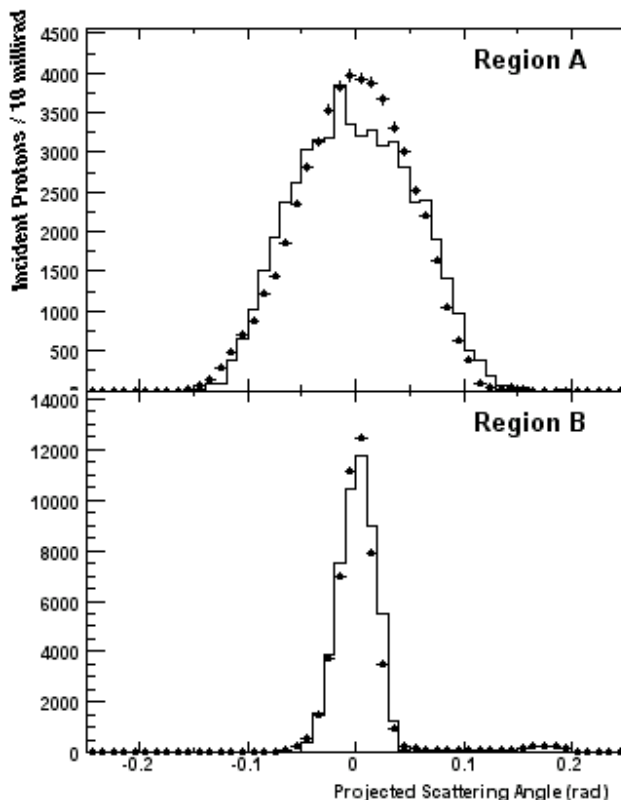


Fig. 7. Comparison of the scattering angle of exiting protons for experiment (points) and simulation (histogram) in regions A and B as indicated in Figures 3 and 4. The area under the histograms was normalized to correspond to the area of the experimental curves.

B. Energy Loss

Protons lose energy in matter mostly through atomic excitation and ionization. This process is well described by the Bethe-Bloch equation. At the energies relevant to pCT, this equation gives the stopping power (i.e. mean rate of energy loss) to be approximately,

$$-\frac{dE}{dx} \propto z^2 \frac{Z}{A} \rho \quad (2)$$

where Z and A are the atomic number and atomic mass of the absorber, z the charge of the incident particle and ρ the specific gravity. [4] Using the information about the wax provided in Sections II-A, the theoretical change in energy of the 250 MeV protons can be calculated. We expect the energy of the protons that have passed through the wax only (region B in Figures 3 and 4) to be approximately 136 MeV while those passing through both the wax and the aluminum (region A in Figures 3 and 4) to be about 57 MeV.

For the experimental energy measurement, the set of cuts outlined in Section II-B were used. For the remaining "good" events, the proton energies at the first detector plane were calculated from the TOT using the calibration curve as explained in Section II-B.

The energy of the simulated protons was recorded at the location of the first detector plane. We again excluded events that did not impact both detector planes, so as to be consistent with the experimental cuts.

As in section IV-A, we considered the data from the protons passing through region A in Figures 3 and 4 separately from those passing through region B. The results are shown in Figure 8.

It is obvious from Figure 8 that the simulation and experimental energy data do not agree as well as the multiple scattering sets. In region B there is a heavy left tail to the experimental data that the simulation does not predict. The existence of this tail seems unusual, as theoretically there should not be this many low energy protons if these protons passed through the wax only. These tail events could be from several sources. First, some of these could be protons that passed through the aluminum and scattered at larger angles before depositing energy in this region. However, since the number of protons scattering at large angles should be small, this is likely only a small portion of these events. It is also possible that these are events in which significant charge sharing occurred, but did not register as having readings in more than one strip. Another possibility is that these events originated from the pile-up of two protons that were registered as a single proton.

There is also a discrepancy in the average energy of experiment and simulation in each region. In region A, the experimental results seem too high, while the simulated results much too low. In region B, though the peaks are closer, the simulated distribution is much more asymmetrical than the experimental. These errors could come from a number of sources. It is possible that the wax and the aluminum are not properly treated in

the simulation, perhaps because their composition and density are not correctly specified. It is difficult, however, to explain the size of the discrepancy in energy loss due to these sources alone. This could indicate errors in the TOT to energy calibration curve. We used an extrapolation of the curve to fit the data. However, there are no calibration points in the range of energies that we are seeing in our experiment, approximately 40-160 MeV, (see Figure 2) so we may not be using the correct calibration at these energies. Another possible source of error could be instabilities in the beam energy, which impact both experimental results and calibration. In addition, the beam may have been contaminated with low-energy protons.

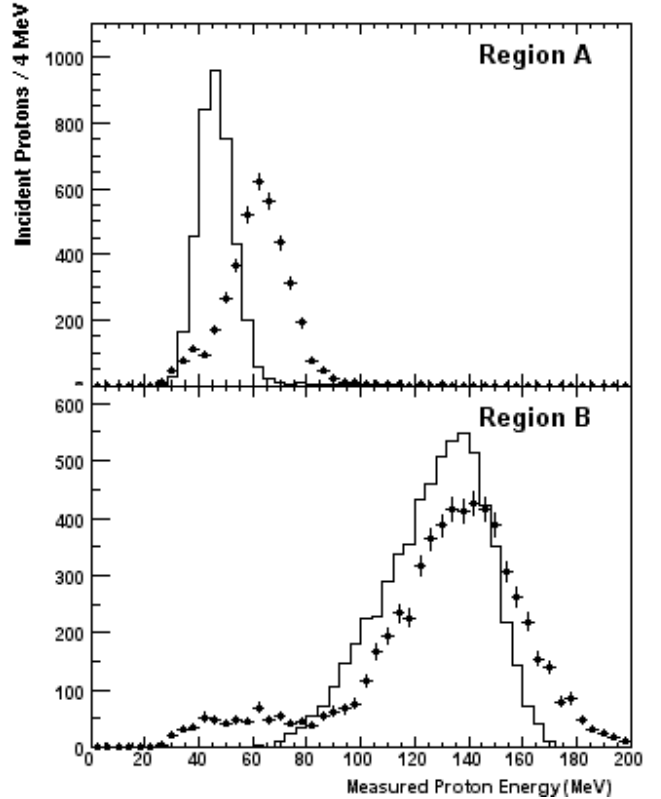


Fig. 8. Comparison of the energy of exiting protons for experiment (points) and simulation (histogram) in regions A and B as indicated in Figures 3 and 4. The area under the histograms were normalized to correspond to the area of the experimental curves.

V. FUTURE WORK

In continuing this work, it is first important to understand the discrepancies between the GEANT4 simulation and experiment. The TOT calibration needs to be evaluated and improved, and calibration in the detectors needs to be performed on a channel by channel basis. The wax and aluminum materials also needs to be examined to determine if we are modeling them properly. We may also need to adjust the modeling of the beam. Once we understand these factors, we can move on to modeling

more complicated experimental setups. First, we will look at an object imbedded in wax and compare this to a corresponding experimental setup. Eventually, we would like to simulate a more complicated phantom, with smaller embedded objects and perhaps with very small density fluctuations like those that typically appear in human soft tissues.

More accurate modeling of the detectors must also be considered in future simulations. In particular, the addition of individual strips of silicon arranged as in the real detector, instead of single planes of silicon, is important so that the simulation more closely resembles the experimental setup. This would also enable us to examine issues such as charge sharing between strips. Additionally, including new types of detectors with better energy resolution will be vital in discovering how to get the best resolution with the lowest dose.

REFERENCES

- [1] Geant4 results and publications, wwwinfo.cern.ch/asd/geant4/geant4.html, 2002.
- [2] A. M. Cormack and Koehler. *Phys. Med Biol.*, 21/4:560–569, 1976.
- [3] E. do Couto e Silva, G. Godfrey, P. Anthony, R. Arnold, H. Arrighi, and E. Bloom *et al.* Results from the beam test of the engineering model of the GLAST LAT. *Nucl. Instrum. Meth.*, A474/1:19–37, 2001.
- [4] K. Hagiwara *et al.* Review of Particle Physics. *Physical Review D*, 66:010001+, 2002.
- [5] K. M. Hanson *et al.* *Phys. Med Biol.*, 26:965–983, 1982.
- [6] U. Scheider *et al.* *Phys. Med Biol.*, 41:111–124, 1996.
- [7] S. Agostinelli *et al.* Geant4: A simulation toolkit. *Submitted to Nucl. Inst. Meth.*, SLAC-PUB-9350.
- [8] M. Goitein. *Nucl. Instrum. Meth.*, 101:509–518, 1972.
- [9] Gabor T. Herman. *Image Reconstruction from Projections: The Fundamentals of Computerized Tomography*. Academic Press, New York, NY, 1980.
- [10] R. P. Johnson, P. Poplevin, H. F.-W. Sadrozinski, and E. Spencer. An Amplifier-Discriminator chip for the GLAST silicon-strip Tracker. *IEEE Trans. Nucl. Sci.*, 45:927–937, 1998.
- [11] B. Keeney, V. Bashkurov, R. P. Johnson, W. Kroeger, H. Ohyama, H. F.-W. Sadrozinski, R. W. M. Schulte, A. Seiden, and P. Spradlin. A silicon telescope for applications in nanodosimetry. *IEEE Transactions on Nuclear Science*, 49(4):1724–1727, 2002.
- [12] D. A. Low and K. R. Hogstrom. *Phys. Med. Biol.*, 39:1063–1068, 1994.
- [13] Hartmut Sadrozinski. Proton Computed Tomography, IEEE MIC 2002 Invited Talk.